Optimal coordination of automated vehicles at intersections with turns

Optimal Coordination of Automated Vehicles at Intersections with Turns

Robert Hult, Mario Zanon, Sébastien Gros and Paolo Falcone

Abstract— **In this paper we address the problem of coordinating automated vehicles at intersections by means of optimal control, and extend earlier work to include vehicles that turns inside the intersection. Turning vehicles requires rear-end collision avoidance relations that are turned on and off as a function of the vehicle state, to capture the departure from one lane and the merger onto another. Such binary decisions are difficult to handle with continuous optimization tools, and typically requires the introduction of integer variables. To keep the problem in the continuous optimization domain, we introduce a smooth, approximate representation of the binary on-off decision. Moreover, for both safety and comfort reasons, turning vehicles are required to limit their velocity while the turn is being negotiated We therefore introduce curvature-based acceleration constraints, which implicitly limits the velocity of the vehicle during the turn, and a comfort promoting term in the objective function. We discuss how the problem is transcribed to a nonlinear program and present simulation results which illustrates our approach. We demonstrate that for most practical problem instances the proposed approximation is exact, and that for problem instances where it isn't, the induced conservativeness is small.**

I. Introduction

The problem of coordinating automated vehicles at intersections has received increasing attention during the last years [1],[17]. The main idea is to use vehicle-to-vehicle/infrastructure (V2X) communication and coordination algorithms to determine the action to take by each vehicle, rather than relying on traffic lights, stop-signs and right-of-way rules. This is projected to enable more fluent traffic and avoid stop-and-go driving, leading to an increase in energy efficiency, reduced congestion and increase the capacity of existing infrastructure [5].

Several authors have proposed algorithms for the intersection problem based on Optimal Control (OC) formulations of the problem, see for instance [13], [12], [3], [19], [11], [14]. The advantages of OC based methods are their ability to use explicitly stated performance metrics and account for the vehicle dynamics, and in some cases, also the ability to explicitly account for constraints (e.g., actuator limitations in the vehicles). The disadvantages are commonly related to computational aspects, as OC-based methods typically requires the on-line solution of optimization problems, which tends to be complex due to the interactions between the vehicles. Part of the complexity is due to the combinatorial nature of the problem, vehicles cross the intersection needs to be determined. In fact, finding *a* feasible solution was for this reason shown to be NP-hard in [2]. Common ways to mitigate the complexity issues (at the cost of introducing sub-optimality) are to use heuristics to find the crossing order [12],[11], to divide the problem into vehicle specific subproblems which can be solved sequentially [3],[19] and to consider specific vehicle dynamics and performance metrics that either admit explicit solutions [19] or simplifying reformulations [14].

In earlier work, we have proposed an OC formulation in which all aspects of the problem are optimized jointly over a fixed time-window. The formulation contains no approximations and no sub-optimality is incurred by sequential decision making. Consequently, when solved exactly, the problem gives *the* optimal solution for the specified objective. In [8] we presented a semi-distributed solution algorithm for simple problem instances under a fixed crossing order. We discussed the application of the formulation to Model Predictive Control (MPC) in [10] and presented results from an experimental validation. In [9], we extended the formulation with nonlinear vehicle dynamics and a general cost and demonstrated its application to Economic Nonlinear MPC under fixed crossing orders. Recently, we also presented an OC based heuristic with which crossing orders can be determined [6] taking the specified objective into account.

In this paper, we extend our OC formulation to incorporate vehicles that make turns in the intersection as shown in Fig. 1a, for problems where the crossing order is given (e.g. from the heuristic in [6]). Turning vehicles requires two issues to be addressed: first, the vehicles must adjust their speed during turns to enforce safety and comfort; second, the Rear-End Collision Avoidance (RECA) must be enforced between the turning vehicle and the vehicles on the destination lane from the time that lane is entered, but not before. Similarly, RECA must be enforced between the turning vehicle and the vehicles on its origin lane until the time that lane is left, but not after. The second issue is relatively easy to handle in sequential schemes such as [3], [19], and was addressed in [18] by letting a vehicle impose RECA with respect to the already computed trajectories of the vehicles before it in the decision sequence. For a vehicle behind a turning vehicle, for instance, the time interval during which RECA should be enforced can be extracted from the (already computed) trajectory of the turning vehicle.

However, for joint optimization schemes, handling RECA conditions for turning vehicles introduces a difficulty: Since the trajectories of all vehicles are computed simultaneously, and the time intervals during which the RECA conditions should be enforced are dependent on the trajectory of the turning vehicle, selecting the time intervals is part of the op-

R. Hult, S. Gros and P. Falcone are with the department of Electrical Engineering at Chalmers University of Technology, Gothenburg, Sweden. {hultr, grosse, pfalc} @chalmers.se. M. Zanon are with IMT School of Advanced Studies in Lucca, Italy mario.zanon@imtlucca.it

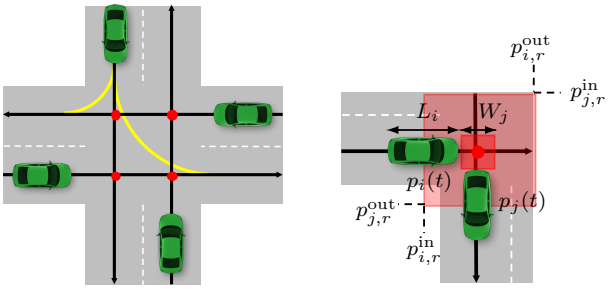

(a) Illustration of the scenarios considered in this paper, with the turning trajectories highlighted in yellow. The collision points for a simple scenario are marked in red.

(b) Illustration of the *collision zone* in light red. L_i and W_i is the vehicle length and width respectively.

Fig. 1: Modeling illustrations

timization problem. In particular, this necessitates constraints that are moved in and out of the problem based on some of the decision variables. Such binary decisions are typically difficult to handle with continuous optimization tools.

The first contribution of the paper is therefore a smooth approximation of the on-off behavior in the RECA constraints for turning vehicles, making it possible to solve the problem using standard methods from continuous optimization. The second contribution is the derivation of curvature dependent acceleration constraints which implicitly limit the vehicle velocity during a turn and enforcing safety. The third contribution is an extension of the energy- and travel time minimizing objective function from [9] to also promote comfortable solutions. We emphasize that we focus on the problem formulation in this paper and do not consider practical solution aspects. A distributed formulation which can be applied in practice is will be the subject of future publications.

The remainder of the paper is organized as follows: In Section II the basic intersection problem is introduced. In Section III, the extensions for turning vehicles are derived and in Section IV, the full OC problem is stated and the transcription to a nonlinear program is described. In Section V, some illustrative examples are given and the paper is concluded with a discussion in Section VI.

II. The Basic Intersection Scenario

The basic scenario contains N_a vehicles approaching an intersection such as that shown in Fig. 1, but where no vehicle makes turns inside the intersection. All vehicles are assumed to be automated and cooperative, and there are no other non-cooperative entities (e.g. bicyclists and pedestrians). The vehicles are assumed to follow fixed, predefined paths, due to which only the motion along these paths is considered. The dynamics of vehicle i are

$$\dot{p}_i(t) = v_i(t) \tag{1a}$$

$$\dot{v}_i(t) = \frac{1}{m_i}\left(\frac{G_i}{r_{w,i}} M_i(t) - F_i^b(t) - F_i^r(t)\right), \tag{1b}$$

where $p_i(t)$ and $v_i(t)$ are the position and velocity of the vehicle center along its path, $M_i(t)$ is the motor torque, $F_i^b(t)$ is the friction brake force and $F_i^r(t) = \rho_i^d v_i(t)^2 + \rho_i^r$ collects the resistive forces. Here, m_i is the vehicle mass, G_i the total (fixed) gear ratio, $r_{w,i}$ the wheel radius and ρ_i^d, ρ_i^r are the drag and rolling resistance coefficients, respectively. We further assume that all vehicles are equipped with electric drives, and subject to constraints

$$0 \le M_i(t) \le \min\left(\frac{P_i^{\max}}{\omega_i(t)}, M_i^{\max}\right) \tag{2a}$$

$$\omega_i(t) \le \omega_i^{\max}, \tag{2b}$$

where $P_i^{\max}$ is the maximum power that can be delivered by the electric motor, $\omega_i(t) = G_i r_{i,w} v_i(t)$ is the electric motor speed, which is upper bounded by $\omega_i^{\max}$ [4]. Moreover, the friction brakes have limited authority and no vehicles reverse in the scenario, so that

$$0 \le F_i^b(t) \le F_i^{b,\max}, \quad 0 \le v_i(t). \tag{2c}$$

A. Collision avoidance

Collisions can occur in and around the intersection, both between vehicles on different lanes and between vehicles on the same lane. Side collisions between vehicles on crossing lanes can occur close to the *collision points*, illustrated with red dots in Fig. 1a. In particular, collisions are possible when more than one vehicle is inside the *collision zone (CZ)*, which is defined as in Fig. 1b. To state conditions for side collision avoidance, we first define the times at which vehicle i enters ($t_{r,i}^{\text{in}}$) and exits ($t_{r,i}^{\text{out}}$) the CZ r as

$$p_i(t_{r,i}^{\text{in}}) = p_{r,i}^{\text{in}}, \quad \text{and} \quad p_i(t_{r,i}^{\text{out}}) = p_{r,i}^{\text{out}}, \tag{3}$$

where $p_{r,i}^{\text{in}}$ and $p_{r,i}^{\text{out}}$ are the entry and exit points of collision zone r on the path of vehicle i. A sufficient condition for collision avoidance is thereby that

$$t_{r,j}^{\text{out}} \le t_{r,i}^{\text{in}} \tag{4}$$

when vehicle j crosses zone r before vehicle j.

Rear-end collision avoidance between vehicles on the same lane is ensured if

$$p_i(t) + \delta_{i,j} \le p_j(t) \tag{5}$$

for vehicle j in front of vehicle i on the same lane, provided that $\delta_{i,j} \ge L_i/2 + L_j/2$, where L_i denotes the vehicle length.

B. Optimal Control Formulation

With the state and inputs of vehicle i as $x_i(t) = (p_i(t), v_i(t))$ and $u_i(t) = (M_i(t), F_i^b(t))$ respectively, we let $x(t) = (x_1, \dots, x_{N_a}(t))$, $u(t) = (u_1, \dots, u_{N_a}(t))$. The OC formulation of the basic intersection problem is

$$\min_{x(t),u(t)} \quad \sum_{i=1}^{N_a} J_i(x_i(t), u_i(t)) \tag{6a}$$

$$\text{s.t.} \quad x_i(0) = \hat{x}_{i,0}, \ (1), (2), \qquad i \in \mathcal{N}, \tag{6b}$$

$$(3), \qquad i \in \mathcal{N}, \ r \in \mathcal{R}_i \tag{6c}$$

$$t_{r,j}^{\text{out}} \le t_{r,i}^{\text{in}} \qquad (i,j,r) \in \mathcal{C}_S, \tag{6d}$$

$$p_i(t) + \delta_{i,j} \le p_j(t) \qquad (i,j) \in \mathcal{C}_R. \tag{6e}$$

where $\mathcal{N} = \{1, \ldots, N_a\}$, $\mathcal{R}_i$ is the set of conflict zones which vehicle i cross and $\mathcal{C}_R$ is the set of vehicle pairs (i, j) such that i, j are on the same lane with j immediately in front of i. The set $\mathcal{C}_S$ is the set of vehicle pairs and conflict zones (i, j, r) such that vehicles i, j are on different lanes which both cross conflict zone r, and vehicle j cross r before i[1]. Finally, the the objective function has the form

$$J_i(x_i(t), u_i(t)) = \phi_i(x_i(t_f)) + \int_0^{t_f} \mathcal{L}_i(x_i(t), u_i(t))\mathrm{d}t, \quad (7)$$

for a fixed final time t_f. For presentational reasons, we postpone the definition of $\mathcal{L}_i(\cdot)$ and $\phi_i(\cdot)$ to Section IV.

III. Introducing Turning Vehicles

In order to model vehicles that make turns inside the intersection and their interaction with other vehicles, the OCP (6) must be extended in two ways. First, constraints must be incorporated to prevent the vehicles from traversing the turns at too high velocities to promote safety. Second, the rear-end collision avoidance condition (5) must be extended for turning vehicles so that a) collision avoidance with respect to the vehicles on the origin lane only is enforced until the turning vehicle leaves the origin lane, and b) collision avoidance with respect to the vehicles on the destination lane only is enforced from the time that the turning vehicle enters the destination lane. We handle both these extensions by introducing additional, nonlinear constraints to (6), which we detail next.

A. Constraining the vehicle velocity during the turn

The forces required to accelerate, brake and turn the vehicle act on the tires. To ensure that the vehicle does not slide during the turn, the combined lateral and longitudinal forces must be limited to lie in what is known as the *adhesion ellipse*. While our approach in principle allows one to constrain the tire forces directly, we instead constrain the acceleration resulting from the forces in order to be consistent with the simple motion model (1). The acceleration constraint is

$$||a_i(t)||^2_{E_i} = \left(\frac{a_{i,lat}(t)}{a^{\max}_{i,lat}}\right)^2 + \left(\frac{a_{i,lon}(t)}{a^{\max}_{i,lon}}\right)^2 \leq 1 \quad (8)$$

where $a_i = (a_{i,lon}(t), a_{i,lat}(t))$, and $a_{i,lon}(t)$, $a_{i,lat}(t))$ are the longitudinal and lateral acceleration, respectively. That is, (8) constrains the acceleration vector to an ellipse with axes of size $a^{\max}_{i,lon}$ and $a^{\max}_{i,lat}$. Provided $a^{\max}_{i,lon}$ and $a^{\max}_{i,lat}$ are chosen small enough considering the tires and road conditions, satisfaction of (8) ensures that the tire forces are small enough for the vehicle to retain traction.

Using the model (1), we have that

$$a_{i,lon}(t) := a_{i,lon}(x_i(t), u_i(t)) = f_{i,v}(x_i(t), u_i(t)), \quad (9)$$

where $f_{i,v}(x_i(t), u_i(t))$ is the right hand side of (1b). While $a_{i,lat}(t)$ is not readily available from the one dimensional motion model used in this paper, we note that the lateral acceleration required to perform a turn is

$$a_{i,lat}(t) := a_{i,lat}(x_i(t)) = \kappa_i(p_i(t))v_i^2(t) \quad (10)$$

where $\kappa_i(s)$ is the curvature at the position s along the turning path. We therefore propose to introduce (8) for all vehicles in (6), using (9) and (10). We remark that (8) limits the longitudinal velocity of the vehicle as it makes the turn through (10).

Definition of $\kappa(s)$: In the current road system, the common practice is to design curved road segments in a piece-wise fashion using clothoidal segments, i.e., segments where the curvature changes linearly along the road, and constant curvature segments, i.e., circle arcs. One motivation for this design is that it yields to changes in the steering angle that are linear in the traveled distance, leading to a linear change in the lateral accelerations for constant velocity turns. In particular, the curvature of a symmetric 90 degree turn starting at a position s_1 along the road is given by

$$\kappa(s) = \begin{cases} \frac{A}{s_2 - s1}(s - s_1) & s \in [s_1, s_2] \\ A & s \in]s_2, s_3] \\ A - \frac{A}{s_4 - s3}(s - s_3) & s \in]s_3, s_4] \\ 0 & s \notin [s_1, s_4] \end{cases} \quad (11)$$

where s_1, s_2, s_3, s_4, and A are such that $s_2 - s_1 = s_4 - s_3$, $s_3 > s_2$ and $\int_{-\infty}^{\infty} \kappa(s)\mathrm{d}s = \pi/2$. We assume that the turning vehicles in the intersection travel on paths which roughly follow this convention. However, to avoid the piece-wise, non differentiable, definition of $\kappa(s)$, we use the following smooth variation of (11)

$$\hat{\kappa}(s) = \frac{A}{2}(\tanh(l\beta(s - \bar{s}_1)) - \tanh(l\beta(s - \bar{s}_2))), \quad (12)$$

where $l = s_4 - s_1, \beta = \frac{A}{s_2 - s_1}, \bar{s}_1 = (s_2 + s_1)/2$ and $\bar{s}_2 = (s_4 + s_3)/2$, which gives that $\int_{-\infty}^{\infty} \hat{\kappa}_i(s)\mathrm{d}s = \pi/2$. An example of both $\kappa(s)$ and $\hat{\kappa}(s)$ is given in Fig. 2a, and corresponding turning trajectories in the global Cartesian frame is given in Fig. 2b. As the figure shows, the $\hat{\kappa}(s)$ yields a trajectory which is very close to that resulting from $\kappa(s)$.

Note that this selection of $\hat{\kappa}$ isn't essential, and that other alternatives are possible. In particular, a vehicle might use the curvature output of a high level, possibly OC based, planner.

B. Conditional Rear-End Collision Avoidance

As illustrated in Fig. 3a, a vehicle i that turns away from lane O onto lane D potentially has four rear-end collision avoidance relations: two with respect to vehicle a and b on the origin lane, formulated as

$$p_i(t) + \delta_{i,b} \leq p_b(t), \qquad t \in [0, t_i^O], \quad (13a)$$

$$p_a(t) + \delta_{a,i} \leq p_i(t), \qquad t \in [0, t_i^O], \quad (13b)$$

where t_i^O is defined as $p_i(t_i^O) = p_i^O$, and p_i^O is the point of departure from lane O, and two with respect to vehicle c

[1]We recall that we only consider problems where the crossing order is given. In a formulation where the crossing order is to be decided, the order of (i, j) in the elements of $\mathcal{C}_S$ is a decision variable. A heuristic method for deciding this order was presented in [6].

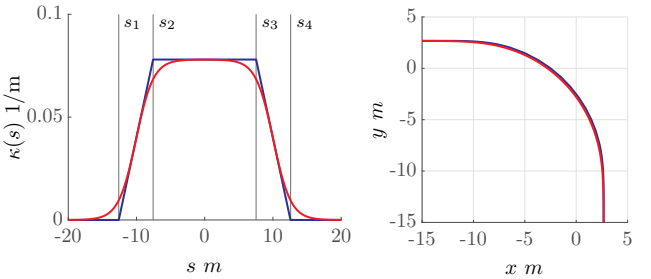

(a) Curvature of the clothoid based turn (11) (blue) and the smooth representation (12) (red).

(b) Illustration of a trajectory in the global fram corresponding to $\kappa(s)$ and $\hat{\kappa}(s)$ of (a).

Fig. 2: Illustration of a turning trajectory

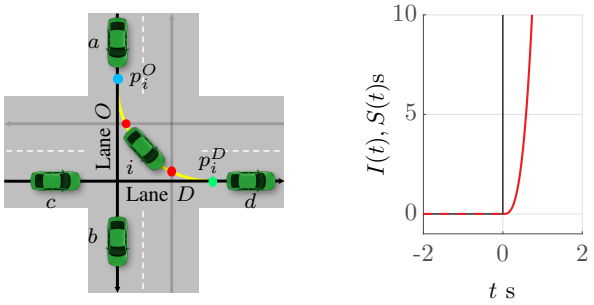

(a) Definitions of vehicles in (13). Conflict points for turning trajectory marked in red.

(b) Illustration of $I(t)$ (black) and $S(t)$ (red).

Fig. 3: Modeling illustrations

and d on the destination lane, formulated as

$$p_i(t) + \delta_{i,d} \leq p_d(t) \qquad t \in [t_i^D, t_f], \tag{13c}$$
$$p_c(t) + \delta_{c,i} \leq p_i(t) \qquad t \in [t_i^D, t_f], \tag{13d}$$

where t_i^D is defined as $p_i(t_i^D) = p_i^D$, and p_i^D is the point of merger with lane D. In terms of the problem formulation (6), this requires the introduction of constraints which are removed from-, and introduced to the problem as a function of the position $p_i(t)$ of the turning vehicle. This type of *"on-off"* relations are difficult to handle with continuous optimization methods, and is often handled by introducing integer decision variables. To keep the problem in the continuous optimization domain, we propose to use a smooth approximation. To this end, we first introduce an equivalent form of (13), exemplified with (13b), where the constraint takes the form

$$p_a(t) + \delta_{a,i} - p_i(t) \leq I(t - t_i^O), \tag{14}$$

where $I(t)$ is the indicator function, defined as

$$I(t) = \begin{cases} \infty & t \geq 0 \\ 0 & t < 0 \end{cases}. \tag{15}$$

The problematic *"on-off"* relation is thereby replaced by a discontinuity in the constraint, equally difficult to handle. In order to avoid the discontinuity, we propose to approximate $I(t)$ with a smooth function and replace (14) with

$$p_a(t) + \delta_{a,i} - p_i(t) \leq S(t - t_i^O), \tag{16}$$

where

$$S(t) = \begin{cases} g(t) & t \geq 0 \\ 0 & t < 0 \end{cases}, \tag{17}$$

and the function $g(t)$ is strictly increasing and such that $g(0) = \dot{g}(0) = \ddot{g}(0) = 0$. An example of $S(t)$ is given in Fig. 3b. Provided that $g(t)$ grows sufficiently fast compared to $p_a(t) + \delta_{a,i} - p_i(t)$, the approximation (16) provides a softened on-off behavior: the constraint is in the problem for all t, but cannot be active for $t < t_i^O$ such that $S(t - t_i^O)$ is significantly larger than $p_a(t) + \delta_{a,i} - p_i(t)$. For t approaching t_i^O, $S(t - t_i^O)$ gradually decreases to a range within which the constraint can be active, and for $t \geq t_i^O$, $S(t - t_i^O) = 0$. Trajectories that satisfy (16) are free of collisions, as formalized in the following proposition:

Propositon 1: If the trajectories $p_i(t), p_a(t)$ satisfy (16), there are no rear end collisions between the turning vehicle i and vehicle a.

Proof: Since $I(t) \geq S(t)$ we have

$$p_a(t) + \delta_{a,i} - p_i(t) \leq S(t - t_i^O) \leq I(t - t_i^O), \tag{18}$$

i.e. if (16) is satisfied, $p_i(t)$ and $p_a(t)$ also satisfy (14) and therefore (13a), which ensures collision avoidance. ■

We note that the set of trajectories satisfying (16) is an inner approximation of the set of trajectories which satisfy (14), which implies that the approximation introduces conservativeness in the collision avoidance condition.

Finally, we remark that side collision avoidance between a turning car and vehicles on crossing paths is handled using (4) and (3) as discussed in Section II-A, using appropriately defined conflict points and zones. Examples of such conflict points are illustrated with red dots in Fig. 3a.

IV. The Full Intersection Scenario

Using constraint (8) and approximation (16), we state the full OCP for intersection problem as

$$\min_{x(t),u(t)} \quad \sum_{i=1}^{N_a} J_i(x_i(t), u_i(t)) \tag{19a}$$
$$\text{s.t.} \quad \text{(6b)} - \text{(6d)}, \tag{19b}$$
$$||a_i(x_i(t), u_i(t)||_{a_i}^2 \leq 1, \qquad i \in \mathcal{N} \tag{19c}$$
$$p_i(t) + \delta_{i,j} \leq p_j(t), \qquad (i,j) \in \mathcal{C}_{RS}. \tag{19d}$$
$$p_i(t_i^O) = p_i^O, \; p_i(t_i^D) = p_i^D, \quad i \in \mathcal{T} \tag{19e}$$
$$R_i(x(t), u(t)) \leq 0 \qquad i \in \mathcal{T} \tag{19f}$$

where $R_i(x(t), u(t))$ collects

$$p_i(t) + \delta_{i,a_i} - p_{a_i}(t) - S(t_i^O - t) \leq 0, \tag{20a}$$
$$p_{b_I}(t) + \delta_{b_i,i} - p_i(t) - S(t_i^O - t) \leq 0, \tag{20b}$$
$$p_i(t) + \delta_{i,c_i} - p_{c_i}(t) - S(t - t_i^D) \leq 0, \tag{20c}$$
$$p_{d_i}(t) + \delta_{d_i,i} - p_i(t) - S(t - t_i^D) \leq 0, \tag{20d}$$

with i being the index of the turning vehicle, relating to vehicles a_i, b_i, c_i, d_i as in Fig. 3a. The set $\mathcal{C}_{RS}$ is the set of vehicle pairs (i,j) such that i,j are on the same lane with j immediately in front of i and where neither i nor j makes a turn.

Objective Function: An Economic cost function for the intersection problem was proposed in [9], with which each vehicle has a specified steady state velocity $v_{r,i}$, and minimizes transient energy consumption. However, it was also noted in [9] that the use of this objective results in high longitudinal accelerations which would be detrimental to passenger comfort. To address this issue, we extend the cost function of [9] and use

$$\mathcal{L}_i(x_i, u_i) = \frac{\omega_i^m M_i}{\eta(x_i, u_i)} - \frac{\alpha_i}{t_f} v_i + \nu_i ||a_i(x_i, u_i)||_{E_i}^2, \quad (21)$$

where we have dropped the explicit time dependence of x_i, u_i, ω_i, M_i and v_i for convenience and . The function $\eta(x_i, u_i)$ is the efficiency map of the electric motor, and the first term is thereby the energy supplied to the electric motor. The second term is a maximization of the average speed (and thereby a minimization of the travel time) with the weighting factor $\alpha_i > 0$. The latter determines the vehicle's steady state velocity $v_{r,i}$ [9] and chosen accordingly. The final term is the addition made in this paper, which penalizes accelerations with the weighting factor $\nu_i > 0$. The latter means that while (8) is a hard constraint on the acceleration, solutions which favor small values will be promoted due to (21). The terminal cost is chosen as

$$\phi_i(x_i(t_f)) = \frac{1}{2}(v_i(t_f) - v_{r,i})^2 P_i \quad (22)$$

where P_i is selected as described in [9]. The solution to (19) using (21) and (22) is thus one where the vehicles have a steady state velocity $v_{r,i}$, and minimizes a trade-off between energy consumption and comfort during the transients.

A. Transcription

To solve the OCP (19) we transcribe the problem to a Nonlinear Program (NLP) using piecewise constant inputs over the time interval Δt and multiple shooting. In particular, the dynamics (1) and constraints (2), (8) are written as

$$x_{i,0} = \hat{x}_{i,0}, \quad (23a)$$
$$x_{i,k+1} = F_i(x_{i,k}, u_{i,k}, \Delta t), \qquad k \in \mathcal{K} \quad (23b)$$
$$0 \geq h_i(x_{i,k}, u_{i,k}), \qquad k \in \mathcal{K} \quad (23c)$$

where $F_i(x_{i,k}, u_{i,k}, \Delta t)$ is the solution to (1) at time Δt with $x_i(0) = x_{i,k}$ and $u_i(t) = u_{i,k}$ for $t \in [0, \Delta t]$ and $\mathcal{K} = \{0, \ldots, N-1\}$. Moreover, the NLP objective is

$$J_i^d(w_i) = \phi_i(v_{i,N}) + \sum_{k=0}^{N-1} \ell_i(x_{i,k}, u_{i,k}) \quad (24)$$

where $\ell(x_{i,k}, u_{i,k})$ is the integration of (21) over $[0, \Delta t]$, $w_i = (x_{i,1}, \ldots, x_{i,N}, u_{i,1}, \ldots, u_{i,N})$ and $N = t_f/\Delta t$ We recall that $t_{r,i}^{\text{in}}, t_{r,i}^{\text{out}}, t_i^O$ and t_i^D are defined implicitly through (3), $p_i(t_i^O) = p_i^O$ and $p_i(t_i^D) = p_i^D$, respectively. With the discretized dynamics (23), a continuous representation of $p_i(t)$ is no longer available, due to which the definitions of $t_{r,i}^{\text{in}}, t_{r,i}^{\text{out}}, t_i^E$ and t_i^D must be modified. To this end, we adopt the approach of [8], and introduce the following representation of the position

$$p_i^d(t, w_i) = F_{i,p}(x_{i,k}, u_{u,k}, \delta t), \ k = \lfloor t\Delta t \rfloor, \ \delta t = t - k\Delta t \quad (25)$$

where $F_{i,p}(x_{i,k}, u_{u,k}, \delta t)$ is the position component of (23b), and note that $p_i^d(t, w_i)$ is twice continuously differentiable in t for w_i satisfying (23). The modified definitions of $t_{r,i}^{\text{in}}, t_{r,i}^{\text{out}}, t_i^O$ and t_i^D are

$$p_i^d(t_{r,i}^{\text{in}}, w_i) = p_{r,i}^{\text{in}}, \quad p_i^d(t_{r,i}^{\text{out}}, w_i) = p_{r,i}^{\text{out}}, \quad (26)$$

and

$$p_i^d(t_i^O, w_i) = p_i^O, \quad p_i^d(t_i^D, w_i) = p_i^D. \quad (27)$$

The discretized formulation of (20) consists of the evaluation of $R_i(\cdot)$ using $p_q(t_k) = p_{q,k}$, $q \in \{i, a, b, c, d\}$,$\forall k \in \mathcal{K}$. We collect the resulting inequality constraints in $R_i^d(w, T_i^R) \leq 0$, where $T_i^R = (t_i^O, t_i^D)$. Using $w = (w_1, \ldots, w_{N_a})$, $T = (T_1, \ldots, T_{N_a})$, where T_i collects $t_{r,i}^{\text{in}}, t_{r,i}^{\text{out}}$, $r \in \mathcal{R}_i$, and collecting all T_i, $i \in \mathcal{T}$ in T^R, the NLP formulation of OCP (19) reads

$$\min_{w,T,T^R} \quad \sum_{i=1}^{N_a} J_i^d(w_i) \quad (28a)$$
$$\text{s.t.} \quad (23), (26) \qquad i \in \mathcal{N} \quad (28b)$$
$$p_{i,k} + \delta_{i,j} \leq p_{j,k} \quad (i,j) \in \mathcal{C}_{RS}, k \in \mathcal{K} \quad (28c)$$
$$t_{r,j}^{\text{out}} \leq t_{r,i}^{\text{in}} \qquad (i,j,r) \in \mathcal{C}_S \quad (28d)$$
$$(27), R_i^d(w, T_i^R) \leq 0 \quad i \in \mathcal{T} \quad (28e)$$

We note that the objective and all constraints are at least twice continuously differentiable, enabling second order methods to be applied to obtain a solution.

V. Simulation Examples

We have evaluated the problem formulation presented in this paper on examples of the type shown in Fig. 4. The NLP (28) was solved using the primal-dual interior point solver in Matlabs native *fmincon*, and utilized ERK4 integrators from the ACADO toolkit [16] for (23b) and (24). The considered scenarios only contained vehicles of the same type with parameters summarized in Table I, $v_r = 70\ km/h$, $a_{lat}^{\max} = 2.5\ m/s^2$ and $a_{lon}^{\max} = 4\ m/s^2$. We used the approximate efficiency map $\eta(\cdot)$ in (21) from [15], which consist of a polynomial fitted to experimental data. The turn was defined such that $s_4 - s_1 = 25\ m$, $s_2 - s_1 = s_4 - s_3 = 5\ m$ and $A = 0.078\ 1/m$. Moreover, we used $\delta_{i,j} = L_i/2 + L_j/2 + \epsilon$, with the safety margin $\epsilon = 5\ m$. and the objective function coefficients α_i and P_i was chosen using the method of [9], and we set $\nu_i = 1$. Finally, we used $\Delta t = 0.1$, $N = 200$, and chose $g(t) = Ct^3$, with constant $C > 0$.

m	ρ^d	ρ^r	$P^{\max}$	$M^{\max}$	$F^{b\max}$	$\omega^{\max}$	G
1500	0.45	0.22	80	250	10	10	7.9

TABLE I: Vehicle parameters. The units are respectively kg, kg/m, kN, kW, Nm, kN, $kRPM$ and G is unitless.

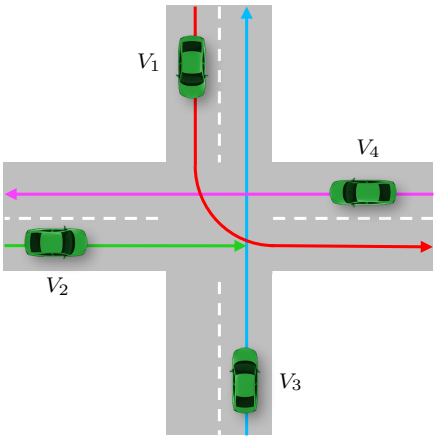

Fig. 4: Example scenario configuration

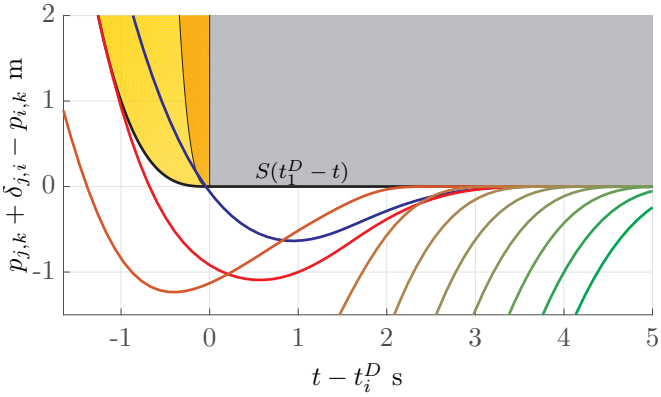

Fig. 5: Illustration of constraint $p_{2,k} + \delta_{2,1} - p_{1,k} \leq S(t_1^D - t)$. The trajectories are the left hand side of the constraint for the configuration studied, ranging from $p_{2,0} = -150$ (green) to $p_{2,0} = -70$ (red). The light and dark blue line shows the $p_{2,0} = -70$ scenario, solved with $C = 50$. The gray area shows the exact constraint resulting from use of $I(t)$, and the yellow area shows the reduction of the feasibility set resulting from the use of $S(t)$ with $C = 1$, and the orange area corresponds to the same with $C = 50$.

A. Illustration of the RECA approximation

To demonstrate the approximation of the RECA constraint (13) in isolation, we considered the scenario where only V_1 and V_2 were present and V_1 turns in front of V_2. We evaluated configurations with initial velocities $\hat{v}_{1,0} = \hat{v}_{2,0} = 70\ km/h$, where the initial position of V_1 was $\hat{p}_{1,0} = -150\ m$ and the initial position of V_2, $\hat{p}_{2,0}$, was varied between -150 to -70 in steps of $10\ m$. In all cases with $g(t) = t^3$ ($C = 1$). The time evolution of $p_{2,k} + \delta_{2,1} - p_{1,k}$ (the left hand side of constraint (20b)) is shown in Fig. 5, together with a representation of the constraint imposed using the indicator function $I(t_1^D - t)$ and that imposed using the approximation $S(t_1^D - t)$ (the right-hand side of (20b)). Since each configuration results in different t_1^D, the time axis is shifted to enable comparisons. Note that the use of $S(t)$ instead of $I(t)$ only results in conservative solutions if the constraint is active for some $t < t_i^O$, i.e., if $p_{2,k} + \delta_{2,1} - p_{1,k} = g(t_1^D - k\Delta t)$ for some k. In the studied examples, this only happens for the case with $\hat{p}_{2,0} = -70$. In the other cases, this does not occur, i.e. the approximation is exact. As can be concluded from the figure, the approximation will only yield conservative solutions when $p_{2,k} + \delta_{2,1} - p_{1,k}$ goes from positive to negative close to t_1^D. Since the velocity of the turning vehicle is limited by (8) this primarily corresponds to scenarios where the rear vehicle is forced to brake hard close to the merge point p_1^D to avoid collisions.

We note that one could obtain a less conservative approximation by increasing the C in $g(t)$. An example where $C = 50$ is drawn in blue in Fig. 3a, for the configuration where $\hat{p}_{2,0} = -70$. As can be seen, $g(t)$ restricts the solution less in this case (c.f. red and blue trajectories), and the resulting trajectory comes closer to that one would obtain using the exact constraint. While the conservativeness is reduced, increasing C is expected to make the problem harder to solve, since it thereby is made more nonlinear. However, this does not seem to be the case in the studied example, in fact the problem is solved faster with $C = 50$.

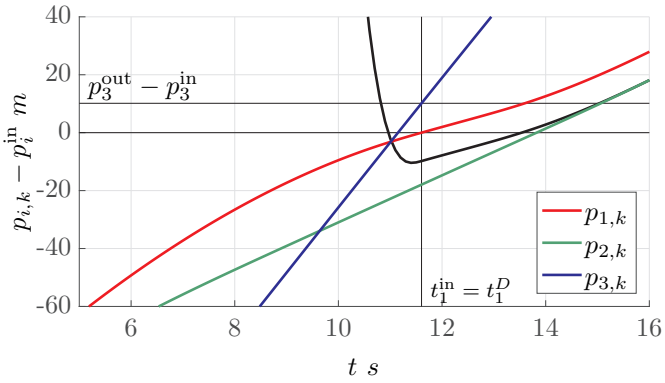

Fig. 6: Position trajectories from the four vehicle scenario of Section V-B. The horizontal bars shows beginning (for V_1 and V_3) and end (for V_3) of the CZ. The black curve is the RECA constraint between V_1 and V_2, as seen from V_2.

B. Illustration of Side CA and acceleration constraints

We evaluated a scenario with V_1 turning and V_2, V_3, V_4 going straight, where the initial velocities were $\hat{v}_{i,0} = 70\ km/h$, $i = 1, \ldots, 4$, and the initial positions were $\hat{p}_{1,0} = \hat{p}_{2,0} = -150$ and $\hat{p}_{3,0} = \hat{p}_{4,0} = -250$. With $V_i \succ V_j$ denoting that V_i crosses a CZ before V_j, the crossing orders were $V_3 \succ V_1$, $V_1 \succ V_2$, $V_4 \succ V_1$, $V_4 \succ V_3$. For simplicity, the merge position on the destination lane p_1^D was taken the same as the start position of the CZ, p_1^{in}. The resulting velocity profiles of all vehicles are shown in Fig. 7 and in Fig. 8 the acceleration is shown for the turning V_1. Fig. 8 illustrates how V_1 brakes into the turn and smoothly transitions into an acceleration out of the turn. The velocity constraint implied by the acceleration limitations through (10) is drawn in black in Fig. 7, and illustrates that V_1 keeps as high velocity as it is allowed when the turn is negotiated.

The position trajectories of vehicles V_1, V_2 and V_3 are shown in Fig. 6, illustrating their crossing of the shared CZ. The figure shows that $p_3(t) = p_3^{\text{out}}$ when $p_1(t) = p_1^{\text{in}}$, thus ensuring that V_1 and V_3 do not collide. The figure also shows the introduction of the RECA constraint between V_1 and V_2,

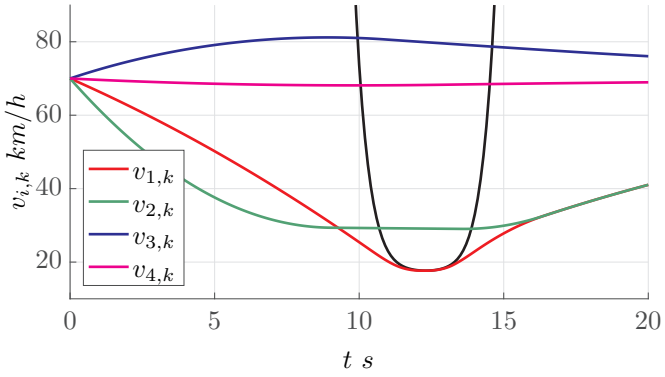

Fig. 7: Velocity trajectories from the four-vehicle scenario of Section V-B. The black line shows the velocity constraint implied by (10) and (8), acting on V_1.

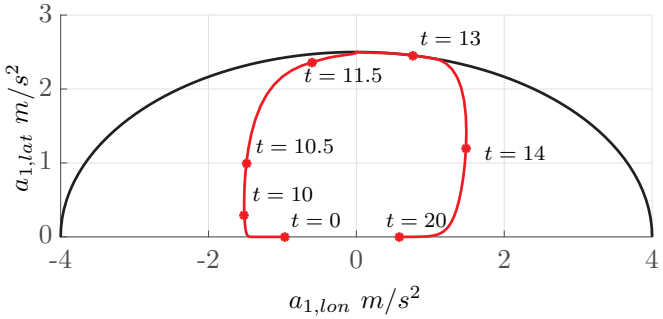

Fig. 8: Acceleration of turning vehicle in the four-vehicle scenario of Section V-B. The black half-ellipse shows the acceleration constraint (8). The red-dotted trajectory is the result from the scenario in Section V-B.

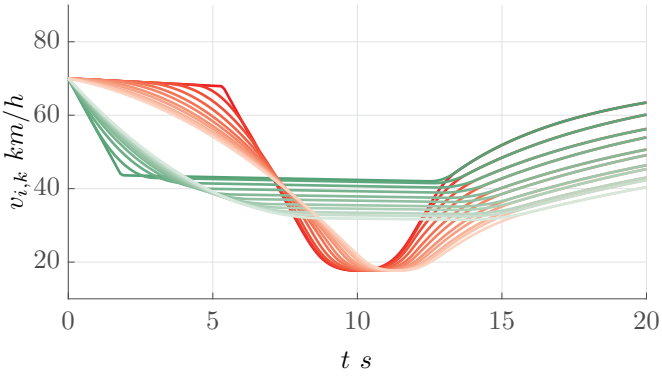

Fig. 9: Velocity trajectories from the two-vehicle scenario of Section V-C. The trajectories correspond values between $\nu = 0$ (dark) and $\nu = 1$ (light) for V_1 (red) and V_2 (green).

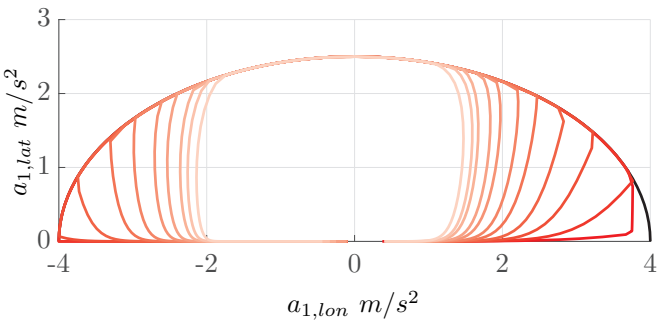

Fig. 10: Acceleration trajectories from V_1 in the two-vehicle scenario of Section V-C. The trajectories correspond values between $\nu = 0$ (dark) and $\nu = 1$ (light).

where $p_{1,k} + \delta_{1,2} - p_{2,k} = 0$ from around 15 s. The effect of the RECA constraint can also be observed in Fig. 7, where V_2 slows down early to arrive after V_1 once it has completed the turn. After after the intersection is crossed, the velocity of both V_1 and V_2 is increased until they converge as the vehicles arrive at the inter vehicle spacing $\delta_{1,2}$. We also highlight the behavior of V_3, which speeds up to prevent V_1,V_2 and V_4 to slow down too much leading to a lower total cost in energy, travel time delay and comfort. An animation of the example can be found at [7].

C. Illustration of the effect of the comfort objective

To illustrate the impact of the "comfort term" in (21), we evaluated a scenario for different values of the weighting factor ν ranging from 0 to 1. The scenario consisted of V_1 and V_2, such that $V_1 \succ V_2$ and $\hat{p}_{i,0} = -150$ m, $\hat{v}_{i,0} = 70$ km/h, $i = 1, 2$, and the resulting velocity and acceleration profiles are given in Fig. 9 and Fig. 10 respectively. As can be seen, $\nu = 0$ leads to aggressive and almost *"bang-bang"* like behavior, with the turning vehicle being at the acceleration limits for almost the entire turn. On the other end with $\nu = 1$, the behavior is much softer, promoting comfort, but achieving a lower average velocity and thus incurring longer travel-time delays.

VI. Discussion and Conclusion

In this paper we have presented an extension to our previous formulation of the intersection coordination problem to include vehicles that take turns. We derived constraints which implicitly limits the velocity with which the vehicles negotiate the turns to promote safety, and introduced a penalization of the total acceleration to promote comfort. Furthermore, we proposed an approximate way to handle the difficult *"on-off"* behaviour of the rear-end collision avoidance constraints associated with turning vehicles.

We emphasize that the conservativeness in the approximate representation of the *"on-off"* constraint (13) can be made small by making $g(t)$ more nonlinear. However, even for less nonlinear choices, conservative solutions resulted only for in extreme cases, where one or both vehicles need to perform aggressive maneuvers close to the merge point to avoid collisions. Due to this, conservativeness would in practice be rare if the problem also includes optimization of the crossing order. Consider e.g. when V_i has to brake heavily to pass after V_j without collision. In configuration, it will likely be beneficial to flip the order and instead let V_i pass before V_j, since the effort spent by both vehicle thereby would decrease.

Moreover, we note that objective function (21) could be developed further by using different penalization for lateral and longitudinal acceleration. In this way the cost could likely be tuned to yield more comfortable trajectories without

suffering to big travel time delays.

We also emphasize that several of the modeling choices used in this paper are not restrictive. For instance, the method easily generalized to scenarios with more than one lane in each direction, there is no requirement on vehicle homogeneity and others vehicle models could be used (for instance, vehicles with ICE powertrains). While the formulation can include more vehicles than four, this was avoided for presentational reasons. The interested reader can find an animated eight vehicle example at [7].

We also emphasize that while the problems tends be more complicated, joint optimization of all parts of the problem will yield a better results than, e.g., a sequential approach. We are currently working on a simulation study to investigate how big the benefits of joint optimization are.

Finally, while we did not discuss the how to solve the problem in a practical setting, we note that simple scenarios that contain no RECA relationships but vehicles that make turns, can be solved with the experimentally validated, semi-distributed method of [8]. A generalization of this method which can handle RECA relationships is the focus of current research.

REFERENCES

[1] L. Chen and C. Englund. Cooperative intersection management: A survey. *IEEE Transactions on Intelligent Transportation Systems*, 17(2):570–586, Feb 2016.

[2] A. Colombo and D. Del Vecchio. Efficient algorithms for collision avoidance at intersections. In *Proceedings of the 15th ACM International Conference on Hybrid Systems: Computation and Control*, pages 145–154, New York, NY, USA, 2012.

[3] G. R. de Campos, P. Falcone, H. Wymeersch, R. Hult, and J. Sjöberg. Cooperative receding horizon conflict resolution at traffic intersections. In *53rd IEEE Conference on Decision and Control (CDC)*, pages 2932–2937, Dec 2014.

[4] L. Guzzella and A. Sciarretta. *Vehicle Propulsion Systems: Introduction to Modeling and Optimization*. 2005.

[5] R. Hult, G. R. de Campos, E. Steinmetz, L. Hammarstrand, P. Falcone, and H. Wymeersch. Coordination of cooperative autonomous vehicles: Toward safer and more efficient road transportation. *IEEE Signal Processing Magazine*, 33(6):74–84, Nov 2016.

[6] R. Hult, M. Zanon, S. Gros, and P. Falcone. An MIQP-based heuristic for Optimal Coordination of Vehicles at Intersections.

[7] R. Hult, M. Zanon, S. Gros, and P. Falcone. Optimal Coordination of Automated Vehicles at Intersections with Turns. `https://youtu.be/DhJ7VJ_Id4o`. [Online: Accessed November 11, 2018].

[8] R. Hult, M. Zanon, S. Gros, and P. Falcone. Primal decomposition of the optimal coordination of vehicles at traffic intersections. In *55th Conference on Decision and Control (CDC)*, pages 2567–2573, Dec 2016.

[9] R. Hult, M. Zanon, S. Gros, and P. Falcone. Energy-Optimal Coordination of Autonomous Vehicles at Intersections. In *Proceedings of the European Control Conference*, 2018.

[10] R. Hult, M. Zanon, S. Gros, and P. Falcone. Optimal Coordination of Automated Vehicles at Intersections: Theory and Experiments. In *To appear in IEEE Transactions on Control Systems Technology*, 2018.

[11] A. Katriniok, P. Kleibaum, and M. Joševski. Distributed Model Predictive Control for Intersection Automation Using a Parallelized Optimization Approach. In *20th IFAC World Congress*, 2017.

[12] K. D. Kim and P. R. Kumar. An mpc-based approach to provable system-wide safety and liveness of autonomous ground traffic. *IEEE Transactions on Automatic Control*, 59(12):3341–3356, Dec 2014.

[13] L. Makarem and D. Gillet. Model predictive coordination of autonomous vehicles crossing intersections. In *16th International IEEE Conference on Intelligent Transportation Systems (ITSC 2013)*, pages 1799–1804, Oct 2013.

[14] N. Murgovski, G. R. de Campos, and J. Sjöberg. Convex modeling of conflict resolution at traffic intersections. In *54th IEEE Conference on Decision and Control (CDC)*, pages 4708–4713, Dec 2015.

[15] N. Murgovski, L. M. Johannesson, and B. Egardt. Optimal Battery Dimensioning and Control of a CVT PHEV Powertrain. *IEEE Transactions on Vehicular Technology*, 63(5):2151–2161, Jun 2014.

[16] R. Quirynen, M. Vukov, M. Zanon, and M. Diehl. Autogenerating Microsecond Solvers for Nonlinear MPC: a Tutorial Using ACADO Integrators. *Optimal Control Applications and Methods*, 36:685–704, 2014.

[17] J. Rios-Torres and A. A. Malikopoulos. A survey on the coordination of connected and automated vehicles at intersections and merging at highway on-ramps. *IEEE Transactions on Intelligent Transportation Systems*, 18(5):1066–1077, May 2017.

[18] Y. Zhang, A. A. Malikopoulos, and C. G. Cassandras. Decentralized optimal control for connected automated vehicles at intersections including left and right turns. In *2017 IEEE 56th Annual Conference on Decision and Control (CDC)*, pages 4428–4433, Dec 2017.

[19] Y. J. Zhang, A. A. Malikopoulos, and C. G. Cassandras. Optimal control and coordination of connected and automated vehicles at urban traffic intersections. In *American Control Conference (ACC)*, pages 6227–6232, July 2016.